Elastoplastic FEM analysis of earthquake response for the field-bolt joints of a tower-crane mast

Yoshitaka Ushio[*1], Tomoharu Saruwatari[2a] and Yasuyuki Nagano[**1]

[1]*Graduate School of Simulation Studies, University of Hyogo 7-1-28 Minatojima-Minamicho, Chuo-ku, Kobe 650-0047, Japan*
[2]*Engineering Technology Div. JSOL Corporation, 2-2-4 Tosabori, Nishi-ku, Osaka, 550-0001, Japan*

Abstract. Safety measures for tower cranes are extremely important among the seismic countermeasures at high-rise building construction sites. In particular, the collapse of a tower crane from a high position is a very serious catastrophe. An example of such an accident due to an earthquake is the case of the Taipei 101 Building (the author was the project director), which occurred on March 31, 2002. Failure of the bolted joints of the tower-crane mast was the direct cause of the collapse. Therefore, it is necessary to design for this eventuality and to take the necessary measures on construction sites. This can only be done by understanding the precise dynamic behavior of mast joints during an earthquake. Consequently, we created a new hybrid-element model (using beam, shell, and solid elements) that not only expressed the detailed behavior of the site joints of a tower-crane mast during an earthquake but also suppressed any increase in the total calculation time and revealed its behavior through computer simulations. Using the proposed structural model and simulation method, effective information for designing safe joints during earthquakes can be provided by considering workability (control of the bolt pretension axial force and other factors) and less construction cost. Notably, this analysis showed that the joint behavior of the initial pretension axial force of a bolt is considerably reduced after the axial force of the bolt exceeds the yield strength. A maximum decrease of 50% in the initial pretension axial force under the El Centro N–S Wave ($v_{max} = 100$ cm/s) was observed. Furthermore, this method can be applied to analyze the seismic responses of general temporary structures in construction sites.

Keywords: elastoplastic analysis; FEM; tower crane; bolted tensile joints; seismic responses; numerical modeling

1. Introduction

Safety measures for tower cranes are extremely important among the seismic countermeasures at high-rise building construction sites. In particular, the collapse of a tower crane from a high position is a very serious catastrophe (Zrnic *et al.* 2011). A typical example of such an accident due to an earthquake is the case of the Taipei 101 Building (the author was project director), which occurred on March 31, 2002. In that accident, two tower cranes collapsed because of failure of the

---

site joints of the tower-crane mast during an earthquake. The amplification effect of the resonance of the tower crane and building and the resulting unexpected load on the joints is regarded as the cause of the collapse.

In the steel structure of a permanent building, the joints of members such as columns, beams, and bracings should be designed with a strength that is greater than that of the jointed members (AIJ Recommendation 2012). However, for temporary structures that are premised on being dismantled, such as a tower-crane mast, the efficiency of site work is taken into consideration, and the joining portion has details that are easy to install and dismantle. However, there are cases in which such joints are not as strong as the joined members. In the case of a huge earthquake such as the Nankai Earthquake, which is expected to occur in the future, and the amplification of seismic loads due to resonance with the building in which a tower crane is installed, it is expected that tower-crane masts may be destroyed by the resulting unexpected load. In that case, it is also expected that the breaking of bolts at the site joints of a tower crane mast will cause a serious disaster, like the one that occurred at the Taipei 101 Building.

Therefore, it is necessary to prevent the collapse of tower cranes by designing and taking measures on the construction site, studying the detailed mechanical behavior of tower-crane mast joints during an earthquake. As for an analysis to obtain the detailed mechanical behavior, it is conceivable to model all of the structural members of a tower-crane mast with solid elements and perform a finite element method (FEM) elastoplastic earthquake-response analysis. However, in the case of seismic-response analysis, the calculation of a large number of steps is required, and considering current computer technology, such an analysis is not realistic in terms of calculation time. Chen *et al*. 2013, Gu *et al*. 2013, and Huang and Syu 2014 have reported on the FEM analysis of tower cranes.

The purpose of this paper was to create a new hybrid-element model (HEM) that not only expressed the detailed behavior of the site joints of a tower-crane mast during a large earthquake but also suppressed any increase in the total model-analysis calculation time and revealed that behavior through computer simulation. The HEM was composed of three element types: beam elements, shell elements, and solid elements. The elastoplastic FEM analysis using HEM in this paper is focused on the modeling on the structure of a tower crane mast, but not on mathematical theory of FEM such as Hybrid FEM. In the proposal, we compare the analysis results between the HEM and beam-element model (BEM), which is composed only of the beam elements and confirms the effectiveness of the proposed model.

2. Destruction of the site joints of the tower-crane mast in the Taipei 101 building

In the afternoon of March 31, 2002, during construction of the Taipei 101 Building, two of the four tower cranes (mast length 48 m, boom length of about 50 m) installed on the 53rd floor collapsed and fell to the ground because of an earthquake, causing serious human injury and damage to the building (Loh *et al*. 2013, Ushio *et al*. 2017). This accident was caused directly by failure of the bolts of the mast joint located just above the horizontal support of the tower crane. One of the cranes fell into an intersection southeast of the building, and the other dropped into a low-rise building under construction to the northwest. Five people, including the two tower-crane operators (all were construction workers), were killed, and about 20 people were injured; the building under construction was also seriously damaged.

Seismographs at three ground-surface locations near the construction site, the maximum accelerations at each of the locations were 193, 100 and 57 Gal, and it is inferred that the

Fig. 1 Scenes of the tower-crane accident in the Taipei 101 Building caused by the earthquake

earthquake was medium, with an acceleration of about 100 Gal. This is supported by the fact that few other buildings in Taipei City collapsed during this earthquake. According to the investigation of causes for this accident, including an analysis of the earthquake response of the tower crane carried out after the accident, it was concluded that "The strengths of the masts of the fallen tower crane satisfied the seismic design standards of Taiwan and Japan, but the collapse of the cranes was due to the destruction of the mast, caused by the amplification effect of the building in which they were installed. The amplified load considerably exceeded the design load." It is known that the difference between the natural periods of a building and tower crane greatly affects the earthquake response of the tower crane, as its height increases during the construction. Due to the amplification effect of the resonance with the building vibrations, the earthquake load applied to a tower-crane mast and temporary support structure may be several times as large as when it is installed on the ground (Ushio *et al*. 2017, Ai *et al*. 2013).

In this paper, a tower crane of the same model as the one that collapsed at the site of the Taipei 101 Building was used in the analysis.

3. Simulation model

3.1 Numerical calculation method

For the calculation, we used LS-DYNA R 9.2.0_Rev. 119543, which was developed by the Livermore Software Technology Corporation (LSTC). This software employs an explicit scheme, and it can calculate large-scale problems at high speed. It is suitable for analyzing nonlinear problems, including those involving large deformations, making it possible to stably calculate buckling and fracture phenomena. Therefore, it is possible to accurately evaluate the collapse of a structure and determine its ultimate proof stress. Furthermore, given that the software can accurately analyze the contact state between parts using its own contact algorithm, it can be used to accurately model and evaluate an assembled structure with bolt joining. Therefore, this software should be suitable for the numerical analysis in this research. One of the recent good examples of this software's application to the architectural engineering field refers to Mizushima *et al*. 2018.

3.2 Modeling of the tower-crane mast

3.2.1 Outline of hybrid-element modeling
To model the tower crane for earthquake-response analysis, it was assumed that the mast was a three-dimensional truss structure and the crane-machine portion (lifting machine, counterweight,
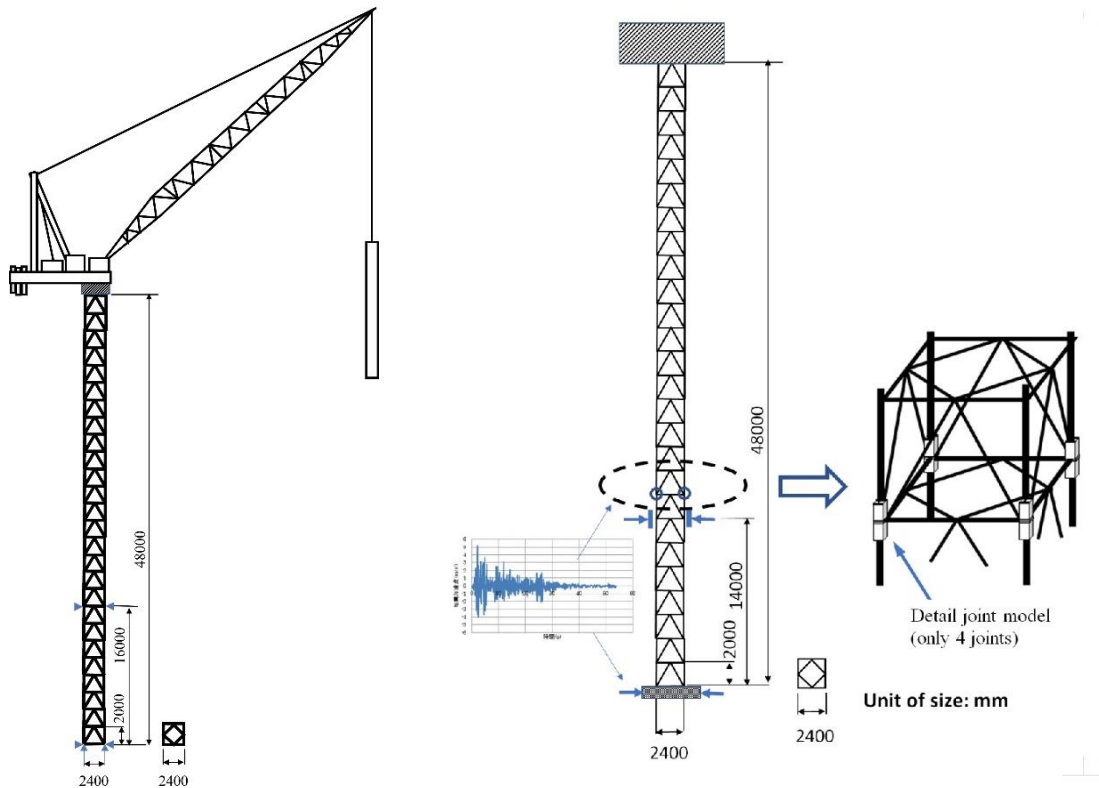
Fig. 2 Image of the analysis model for the FEM dynamic elastoplastic analysis of the tower crane

boom, sling wire, etc.) at the top of the tower crane was installed as one combined mass at the top of the mast structure. As shown in Fig. 2, in the HEM, detailed modeling was performed on the most-critical four site joints near the position of horizontal support. Each site joint was assumed as a beam element composed of two end plates. When designing this modeling, we considered the computing ability of the supercomputer of the University of Hyogo.

In the 3D truss structure of the tower-crane mast, it was assumed that the entire joint system of the post members, vertical bracings, horizontal bracings, and horizontal members (beams) was joined rigidly, and the brace and the horizontal members were connected eccentrically to the post members. Details of the joints of the actual tower crane are shown in Fig. 4.

3.2.2 Modeling the joint part in the HEM

Outline of modeling of the tower-crane site joint

The joint part, as shown in Fig.5, was the same shape as in the model, analyzed using the static elastoplastic FEM, and the site-joint part of the tower-crane mast post was cut out at 450 mm above and below the joining face; the length was 900 mm. This length was determined as three times the width of the post members in consideration of the possibility of analysis when the reinforcing members of the joint part were applied. As for the shape of the joint, the post was H-shaped steel (H-305 × 305 × 10 × 15), the bolt was a large-diameter hexagon bolt M45 × 4, and the thickness of the end plate was 50 mm.
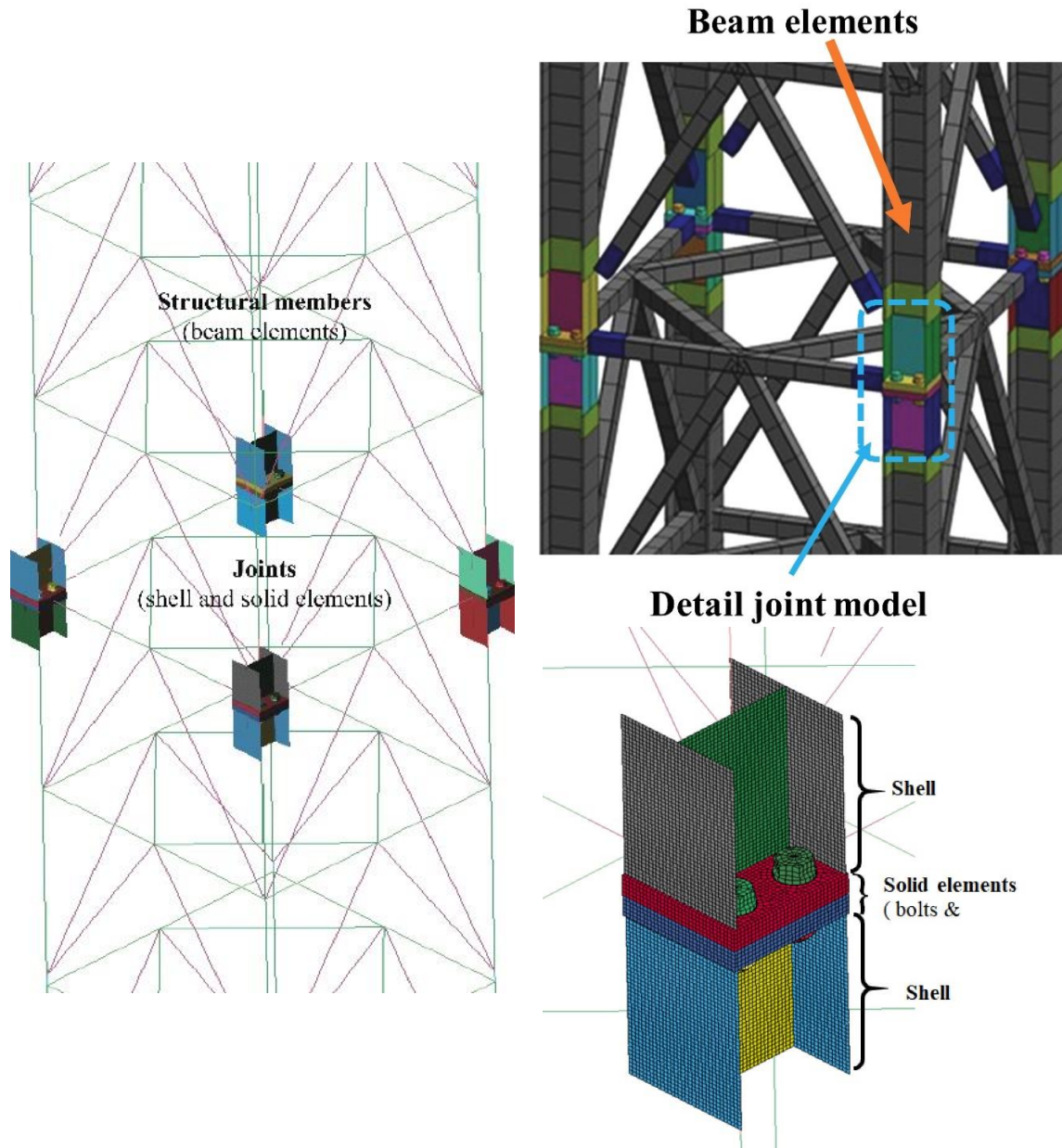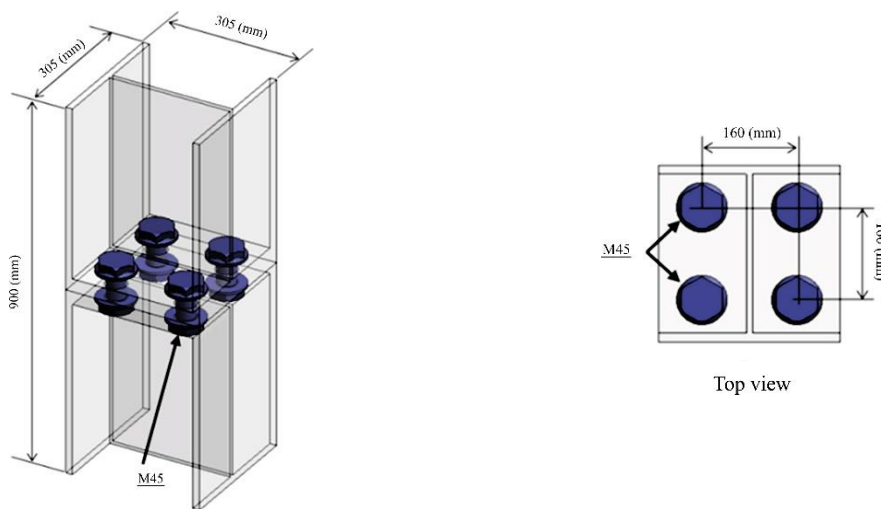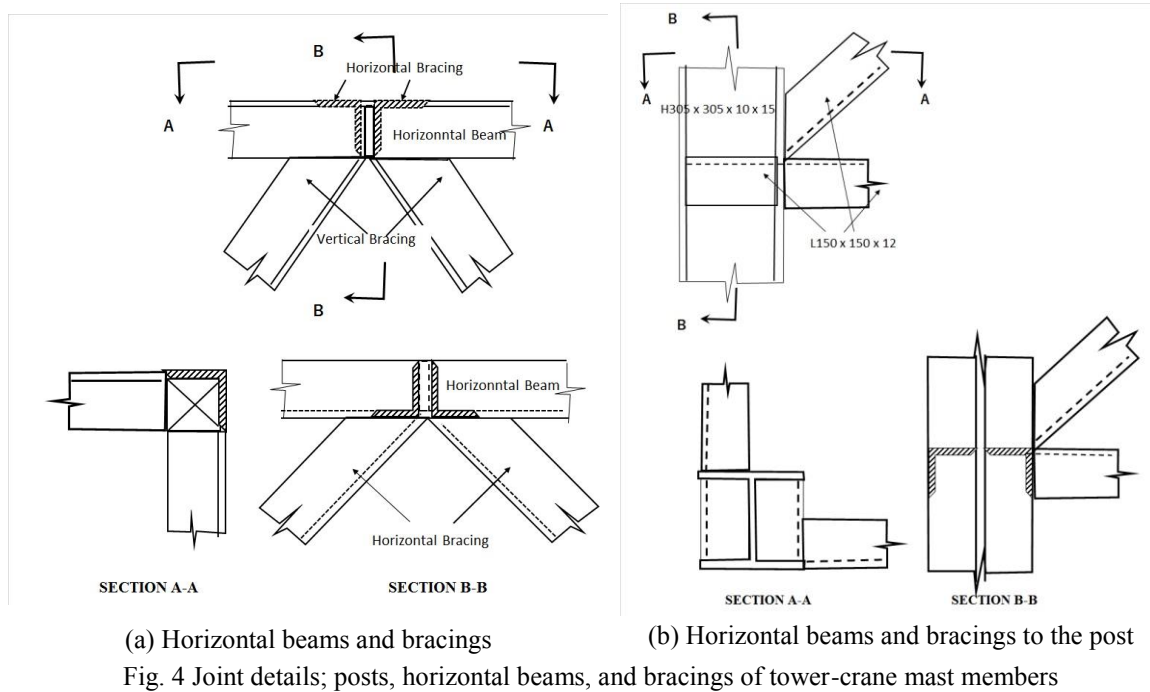
Fig. 3 Modeling of the tower-crane mast (three-dimensional truss and end-plate type bolted site-joint)

Initially, the earthquake-response analysis assumed that a joint-analysis model with the solid-element subdividing system was applied at the four joints and that the other members of the 3-D truss of the tower-crane mast were composed of beam elements. However, after estimating the computer calculation time, it was found that it would take >2000 h, which was not a reasonable amount of time. Therefore, we modeled the joint portion by introducing the new concept of the hybrid system with computer calculation time of about 50 hours using the super computer owned by the University of Hyogo.

(a) Horizontal beams and bracings

(b) Horizontal beams and bracings to the post

Fig. 4 Joint details; posts, horizontal beams, and bracings of tower-crane mast members

Fig. 5 Outline of the joint model

As shown in Fig. 3, the modeling assumed that the post part (450 mm above and below) made of H-shaped steel (H305 × 305 × 10 × 15) was the shell-element model and the end plates and bolts were the solid-element models for the joint parts. The subdividing of the solid-element model was rougher than in the case of the static elastoplastic FEM analysis. The element size was based on a cube with 10 mm sides. The end plates, comprising solid elements, and the post, composed of shell elements, were rigidly joined. The numbers of elements and nodes of HEM and BEM are shown in Table 1.

Table 1 Structural system and number of elements of each part of the joint

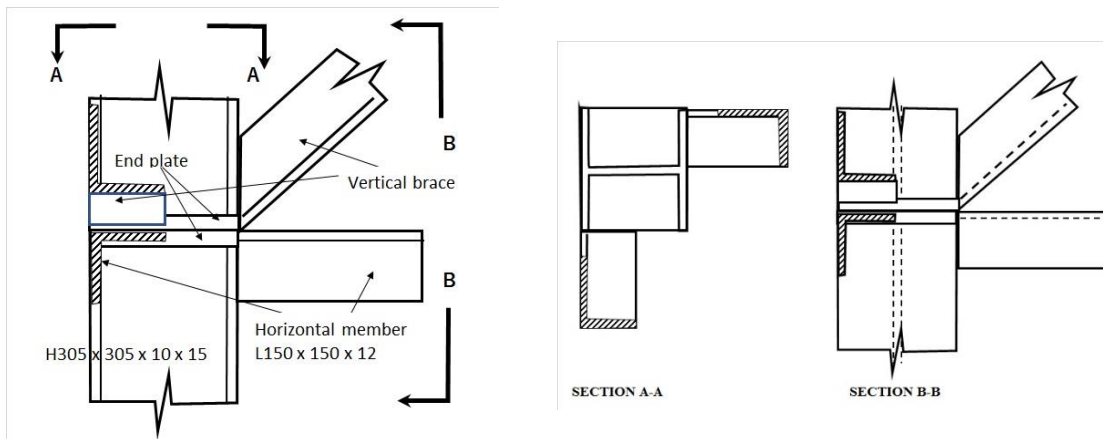| Type of Model	Nodes	Beam elements	Shell elements	Solid elements
HEM	93,897	4,816	30,080	45,952
BEM	4,497	4,856	-	-

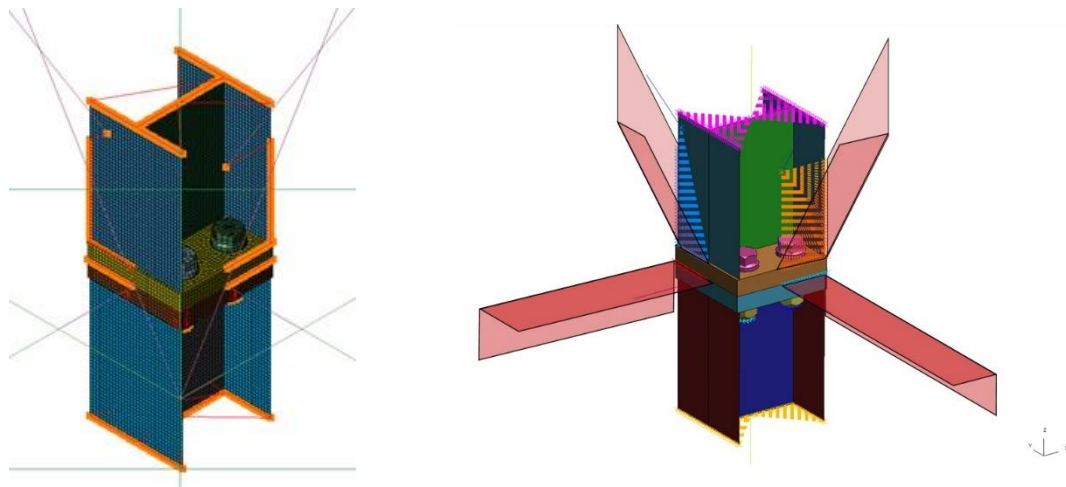Fig. 6 Detail of a site-joint of the actual tower-crane mast

Fig. 7 Modeled connections between the end-plate-type bolt joint, horizontal members, and vertical bracings

Contact condition

The bolted joint connecting members were modeled in as real a situation as possible by defining the contact conditions at the surface between the end plates welded to the upper and lower posts and between the washers and end plates. The contact conditions were controlled by the "constrained method" using the contact determination function (*CONTACT_AUTOMATIC_SURFACE_TO_SURFACE) (LS-DYNA KUM I, II) included in the software. The friction coefficient for these contact surfaces was assumed to be 0.1.
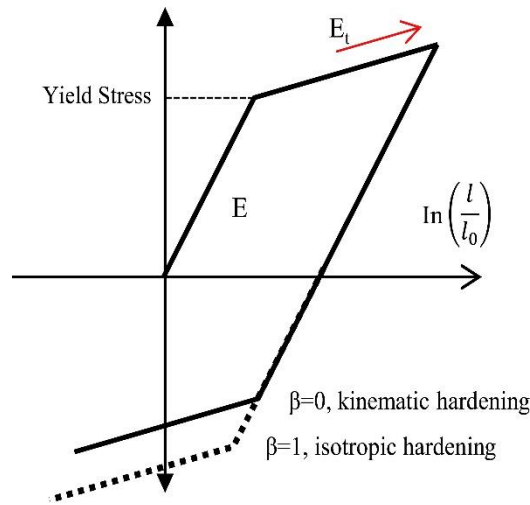
Fig. 8 Hardening

Table 2 Properties of steel materials

	Young's Modulus (MPa)	Density (ton/mm³)	Poisson's Ratio	Yield Strength (MPa)
Post, end plates	2.06×10^5	7.89×10^9	0.3	340
Bracings beams	2.06×10^5	7.89×10^9	0.3	250
Bolts	2.10×10^5	7.89×10^9	0.3	900

Modeling of the site joint to the horizontal members and bracings

The horizontal members and vertical bracings, which were assumed to be composed of beam elements, were connected to the site joints, as shown in Fig. 6. These connections were modeled during this analysis so that the horizontal members and the vertical bracings were eccentrically connected to the end plates and flange/web of the H-shaped steel posts similar to the actual joints. Moreover, the edges of the BEM and shell-element model or solid-element model were connected using *CONSTRAINED_NODAL_RIGID_BODY" (LS-DYNA KUM I, II) with a length corresponding to the width of the horizontal member and bracing, as shown in Fig. 7.

3.2.3. Material model

An elastoplastic material model (*MAT_PLASTIC_KINEMATIC) (LS-DYNA KUM I, II), which is included in the software and considers kinematic hardening, was used for the modeling of material properties. In this model, it is possible to obtain both kinematic ($\beta = 0$) and isotropic hardening ($\beta = 1$) by setting the hardening parameter β ($0 < \beta < 1$). In this analysis, kinematic hardening ($\beta = 0$) was used.

It is also possible to consider the fracture behavior after yielding, which was used for modeling the general metal materials, composite materials, plastics, and similar materials. Although it was also possible to consider the influence of the strain rate, no shock load was applied in this analysis; therefore, it was excluded. Furthermore, the breakage of elements was not considered. Table 2 lists the properties of the materials used.
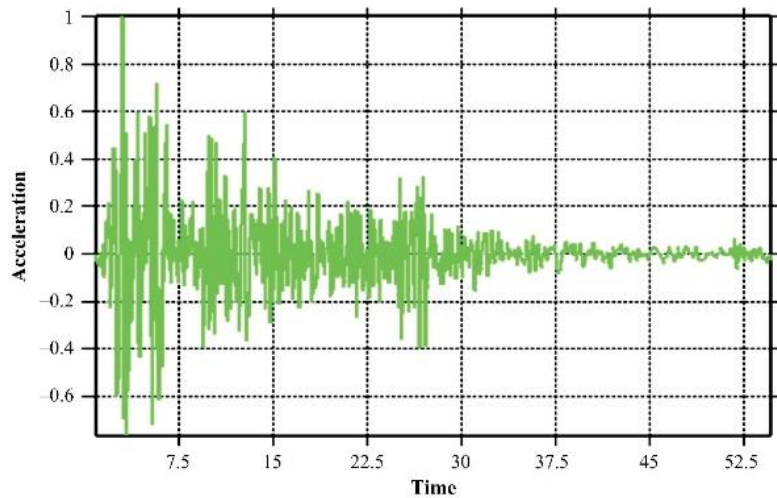
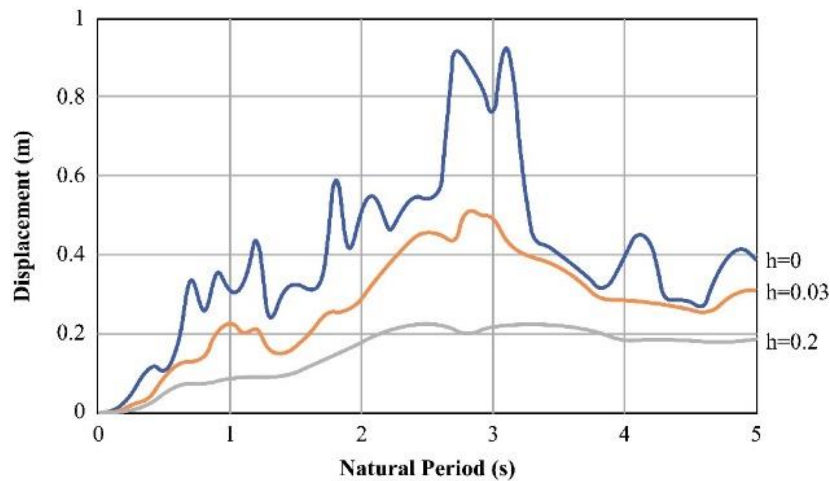Fig. 9 Acceleration history of El Centro N–S waves

Fig. 10 Displacement spectra of El Centro N–S waves

3.3 Earthquake loading

The seismic force ELCENTORO - NS (v_{max} = 100 cm/s) was applied as the seismic loading on the bottom of the mast supporting the tower crane and at the horizontal support located 14 m above the base, as shown in Fig. 1. As mentioned above, considering the resonance of the building under construction and the tower crane, we used an earthquake strength twice as large as Japanese design seismic-intensity level 2 (v_{max} = 50 cm/s). The El Centro N–S seismic waves and their displacement response spectra are shown in Figs. 9 and 10. The damping ratio of the mast structure is assumed to be 3%, which is slightly high; however, it was determined by referring to the section 5.2.4.3 of JCAS 1101-2018, which describes that "the damping ratio of crane structures is 0.025 for welded structure, 0.04 for bolted structures, and 0.03 for welded and bolted structures."
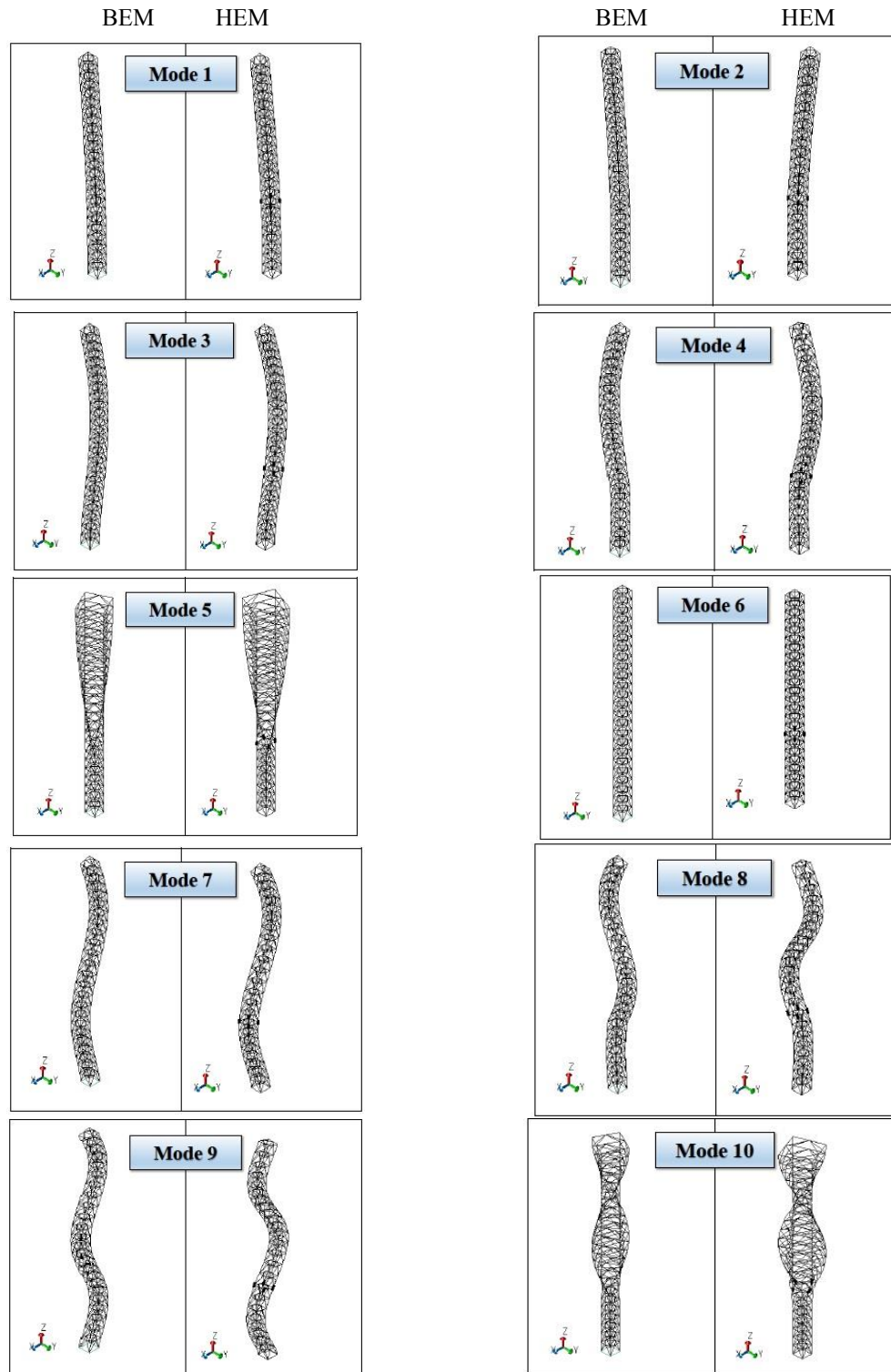
Fig. 11 Mode shapes of BEM and HEM

Table 3 Natural frequency of each mode (Hz)

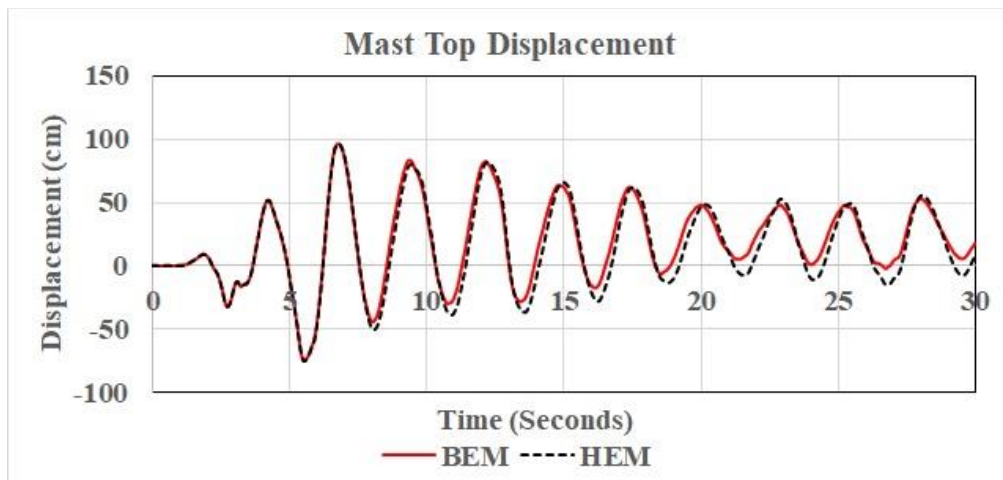| Mode	BEM	HEM	Mode	BEM	HEM
1	0.311	0.330	6	6.93	6.93
2	0.403	0.410	7	10.8	10.8
3	3.99	4.06	8	16.6	16.7
4	6.03	6.11	9	18.9	19.0
5	6.57	6.51	10	19.7	19.5

Fig. 12 Displacement history of the tower-crane top (BEM and HEM)

4. Analysis results

4.1 Comparison of analytical results of BEM and HEM

4.1.1 Natural frequency and vibration mode of the tower crane

The natural frequencies of the tower crane obtained from BEM and HEM are shown in Table 3 up to the 10th-order mode, and the vibration modes are shown in Fig. 11. It was confirmed that there should be no problem with the various structural assumptions in the HEM creation because there was almost no difference between the natural frequencies and eigenmodes of both models.

4.1.2 Comparison of displacement and acceleration history of the top of the tower-crane mast

Figures 12 and 13 compare the displacement and acceleration histories of the top of the tower-crane mast between the BEM and HEM. Although the influence of plasticization of the joint is somewhat observed in the HEM, the seismic response of the tower-crane mast is almost the same, and it seems that there is no problem with the structural assumption in the creation of the HEM.

4.1.3 Comparison of axial forces applied to a joint

The beam element (blue bold lines) of BEM and its number at the location of a site joint are shown in Fig. 14, and those of the detailed modeled joints in the HEM are shown in Fig. 15. The beam elements (one-dimensional of the joints in BEM connect rigidly to the members such as
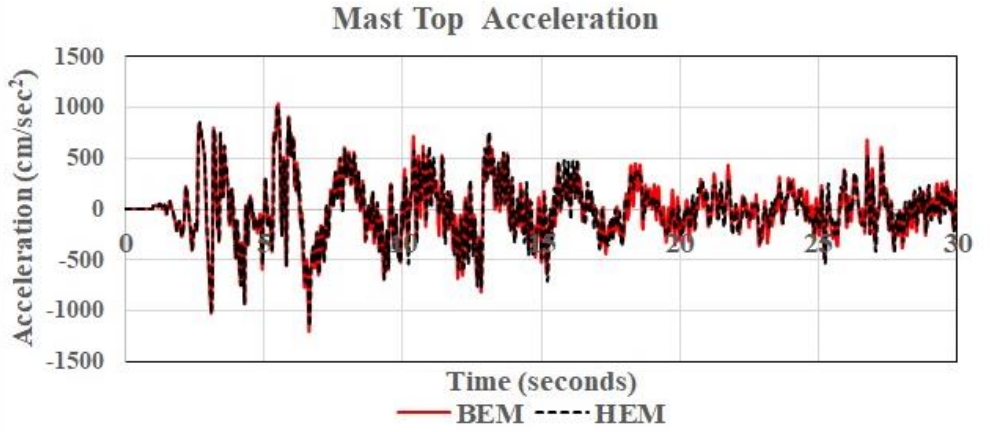
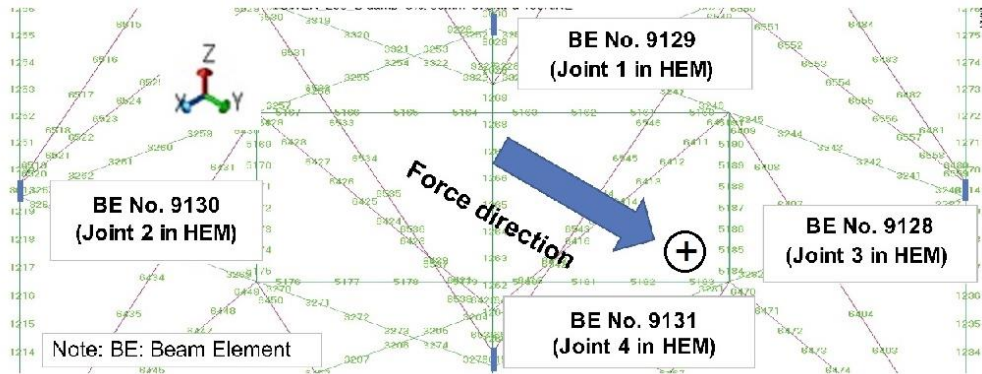Fig. 13 Acceleration history of the tower-crane top (BEM and HEM)

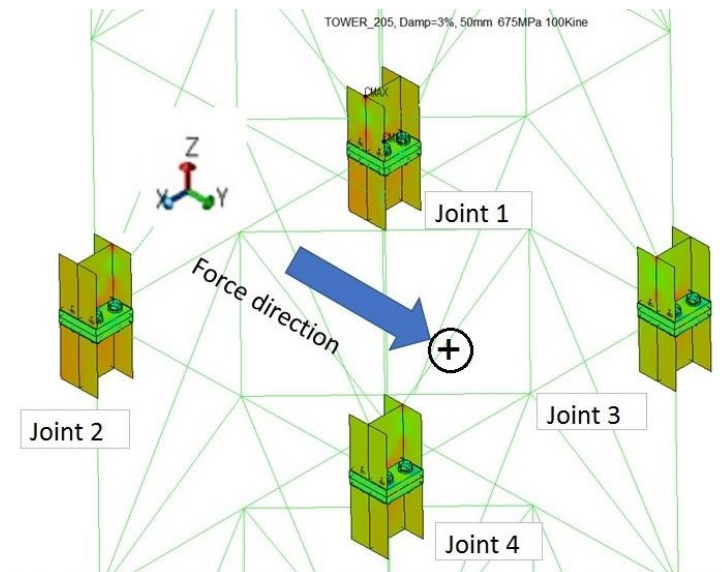Fig. 14 Beam-elements of the joints and their numbers in the BEM

Fig. 15 Detailed model joints and their numbers in the HEM
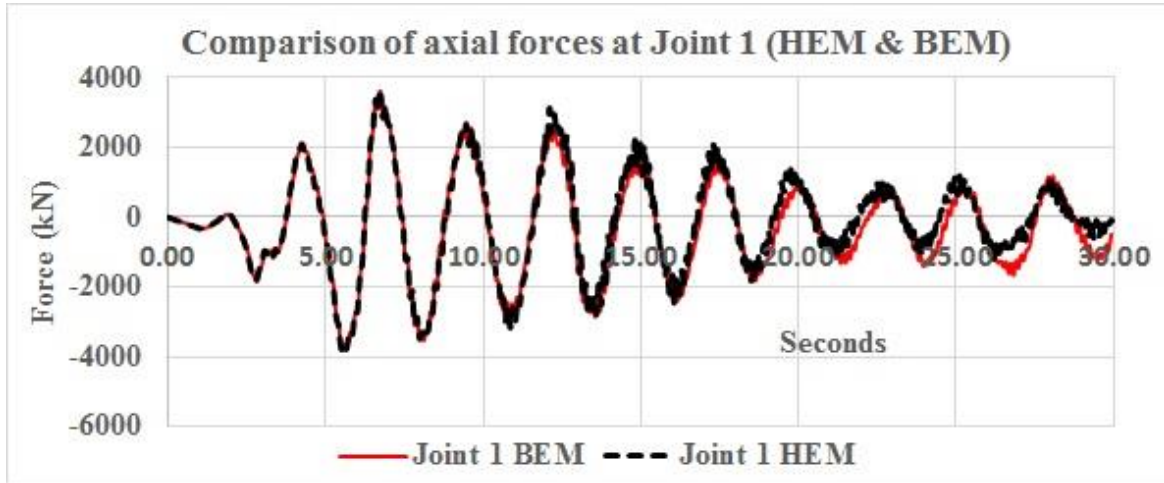
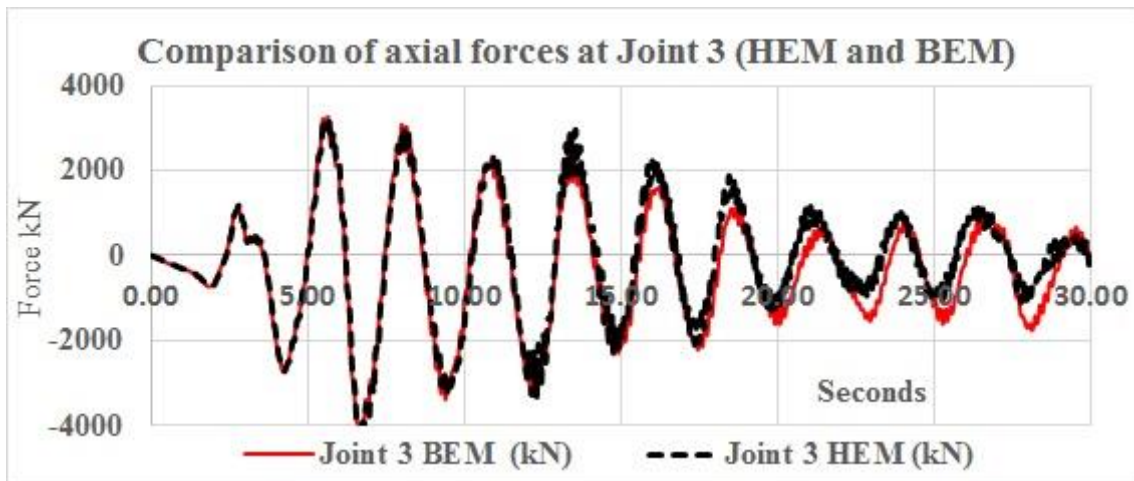Fig. 16 Comparison of axial forces between HEM and BEM at Joint 1

Fig. 17 Comparison of axial forces between HEM and BEM at Joint 3

posts, beams and bracings. Figures 16 and 17 compare the axial forces applied to the joints at beam-element numbers 9129 and 9128 of the BEM and at Joints 1 and 3 of the HEM. The two joints have similar time-related response of axial forces obtained from BEM and HEM. Given that the seismic force is loaded in the y-direction and the shape of the mast is symmetrical, Joints 1 and 2 and Joints 3 and 4 have almost the same response. Therefore, only the responses of Joints 1 and 3 are shown in the two figures.

4.2 Earthquake-response results at joints of hybrid-element model

4.2.1 Changes in bolt and joint axial forces

Figures 18 and 19 show the time-response histories of the axial forces per one bolt in the z-direction of Joints 1 and 3 and the axial force in these bolts. The initial pretension axial force of each bolt is 75% of the yield strength of the bolts. The bolt tensile axial force slightly exceeds the
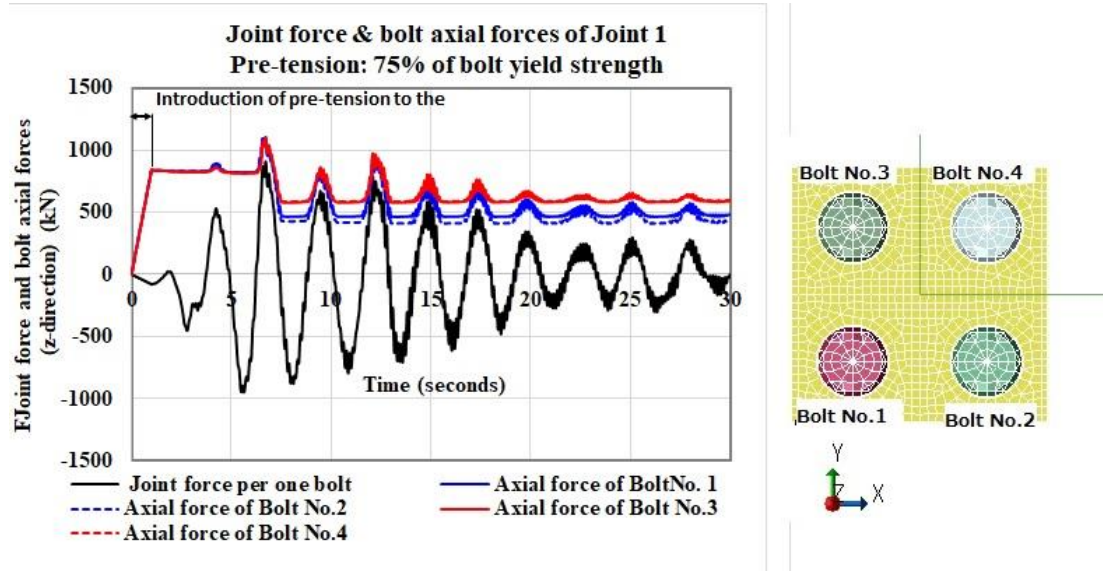
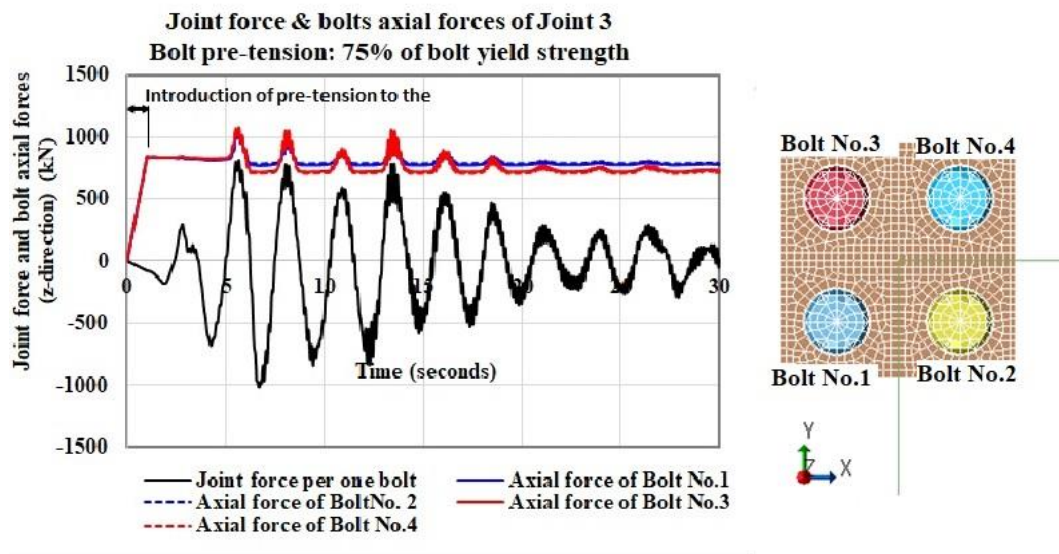Fig. 18 Responses of bolt axial force and joint force on Joint 1

Fig. 19 Response bolt axial force and joint force on Joint 3

initial tension axial force at 4.23 and 3.33 s of the first tension peak and shows the highest value at 6.72 and 5.5s of the second tension peak at Joints 1 and 3, respectively. Notably, the initial pretension axial force of each bolt decreases after the second tension peak of the joints wherein the axial forces of these bolts considerably exceed their yield strength and remains constant as far as the bolt forces are within elastic range. Bolt No. 1 and No. 2 of Joint 1 as well as Bolt No. 3 and No. 4 of Joint 3 located outside the crane mast in the y-direction, which is the direction of earthquake loading, show higher force with more decrease in the initial pretension force compared

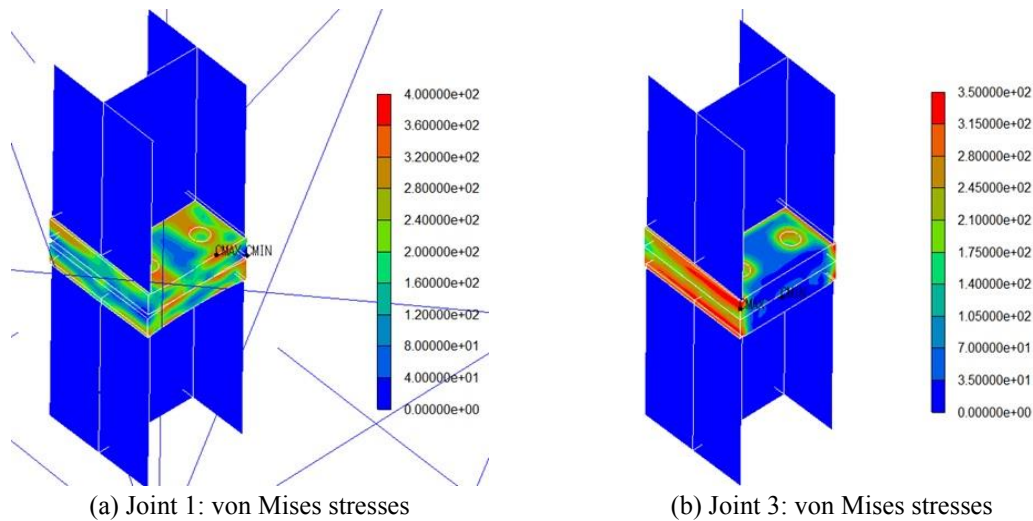(a) Joint 1: von Mises stresses   (b) Joint 3: von Mises stresses

Fig. 20 Contour plot of the von Mises stress for Joints 1 and 3 at 6.72 s

with the other bolts after yielding. The initial pretension force of Bolt No. 1 and No. 2 of Joint 1 as well as Bolt No. 3 and No. 4 of Joint 3 decrease by ~50% and ~15%, respectively. This implies that the extent of bolt yielding may have significant impact on the decrease in initial pretension forces and may cause bolt failure.

4.2.2 Von Mises stress distribution of each part of the tower-crane mast joints

At Joint 1 and Joint 3, the maximum applied tensile forces are 3635 and 3171 kN at 6.72 and 5.5 s, respectively. Figure 20 shows the contour plot of the von Mises equivalent stresses of the end plates in Joints 1 and 3 at 6.7 s. Because Joint 3 is compressed onto the end plate that is not bent, the stresses of the elements around the joints to the flanges of H shape post are large due to compression. Further, at Joint 1, tension is applied to the joint portion, bending stress is generated in the end plate, and the von Mises equivalent stresses are large in the elements on the bolt lines parallel to the flange of the mast post.

Figures 21 and 22 show the contour plots and time-related responses of the von Mises equivalent stresses in the end plates and bolts. From these figures, the detailed earthquake response of the components of the end-plate tension-bolt joint can be understood.

Figures 21 (a) and (b) show the von Mises stress contour plots of end-plate solid elements and the time-related responses of von Mises stresses of six end-plate solid elements with high stress in Joint 1, respectively. This end-plate is the lower part of the two end plates, and Fig. 21 (a) details the end-plate deformation response for better comprehension. Figure 21 (b) shows the joint force per one bolt as black dotted lines for reference. When the joint force becomes the largest at about 6.7 s, the stresses of the six elements of the end-plate exceed their yield strength (340 kN/mm^2). After this peak, the stresses become peak value when the joint is compressed possibly due to the plastic deformation of the end-plate when the joint is subjected to maximum tension force at about 6.7 s.

Figures 22 (a) and (b) show the von Mises stress contour plots of bolt solid elements during peak loading (6.7 s) and the time-related responses of von Mises stresses of three bolt solid elements in Joint 1, respectively. Figure 22 (a) also shows the deformation of bolt in detail. As
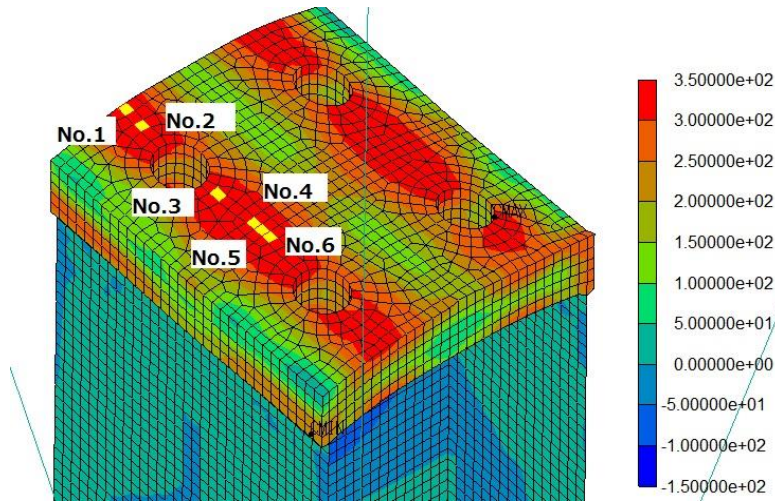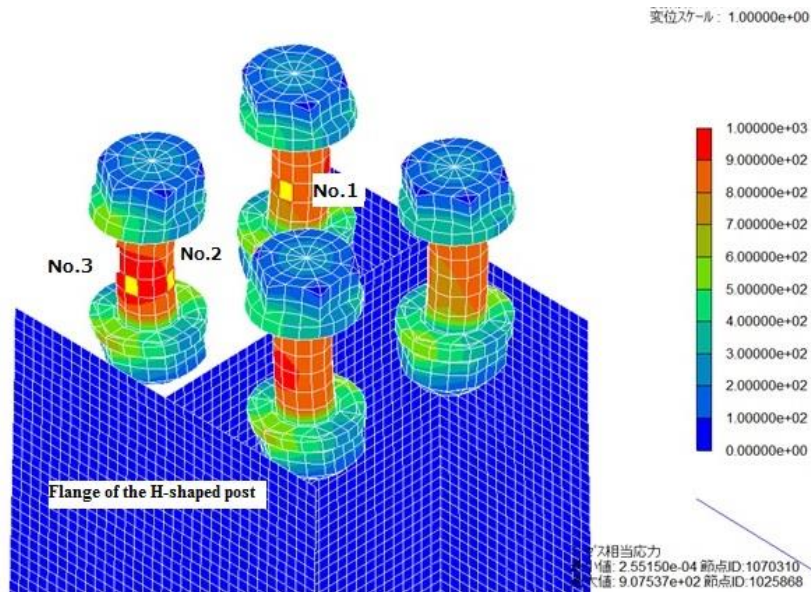
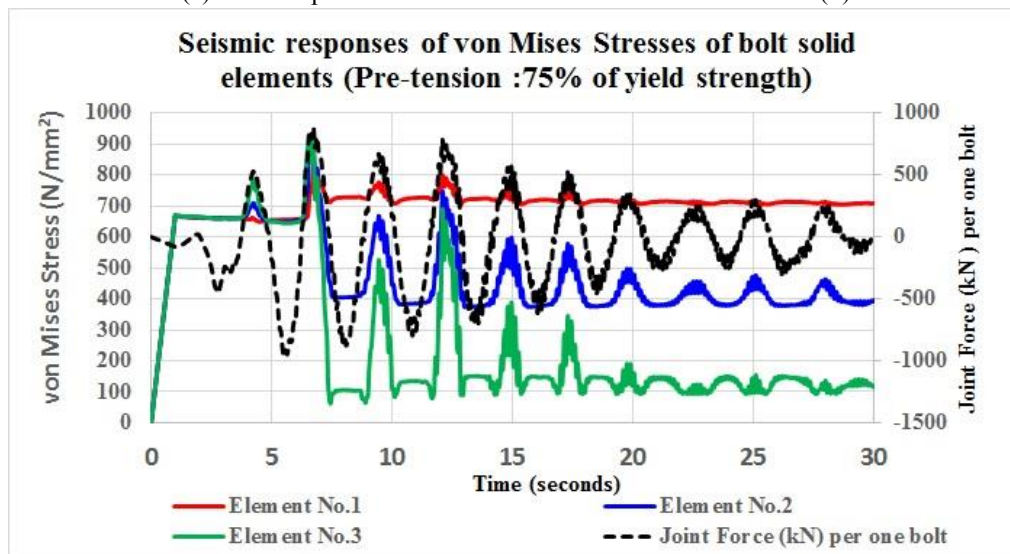(a) End-plate von Mises stress contour plots and the solid-element numbers
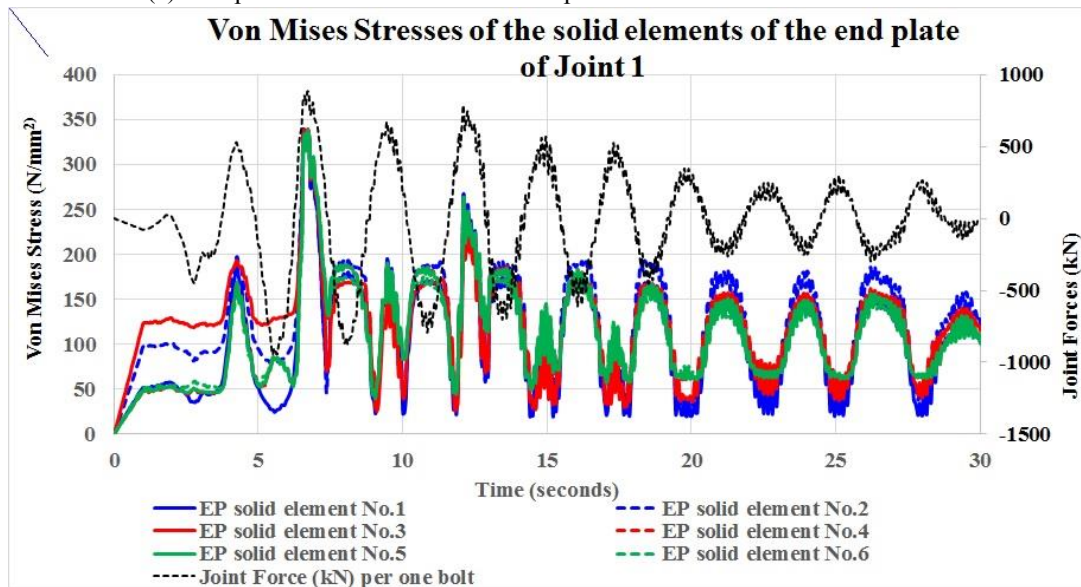
(b) Time-related responses of von Mises stress of the solid elements of an end-plate

Fig. 21 Contour diagram and von Mises stress in the solid elements of an end plate

shown in Fig. 22 (a), the solid elements of bolts facing the flange of H-shaped post have higher von Mises stress which means bending moment is generated in the bolts. Figure 22 (b) also represents the joint force per one bolt as black dotted lines for reference. When the joint tensile force becomes the largest at about 6.7 s, the stresses of No. 2 and No. 3 elements of the bolts exceed their yield strength (900 kN/mm^2). After this peak, the pretension stresses decrease to a certain value and remain constant as long as the stresses do not exceed their yield strength. Conversely, the stress of No.1 element is maintained almost within the elastic range, without any decrease in the initial pretension stress. These results are consistent with those of Fig. 18 and indicate that the bending of bolt shaft must be considered for the design of end-plate bolted joints.

(a) Contour plots and solid-element numbers of the bolts in (b)

(b)

Fig. 22 Contour diagram and von Mises stress in the solid elements of the bolts

4.2.3 The gap between the two end plates and the principal stress vectors of the bolts and end plates

Figure 23 (a) shows, as results of the analysis, the principal stress vectors generated in the end plates and bolts when the largest gap between the two end plates is caused by the tensile load. Figures 23 (b) and (c) show the gap and time-related response of the gap sizes compared with the joint force indicated in black dotted line. These simulation results show the stress distribution of end plates and bolts and the relation of size of a gap between the two end plates and joint forces.

(a) Principal stress vectors

(b) Gaps between the two end plates

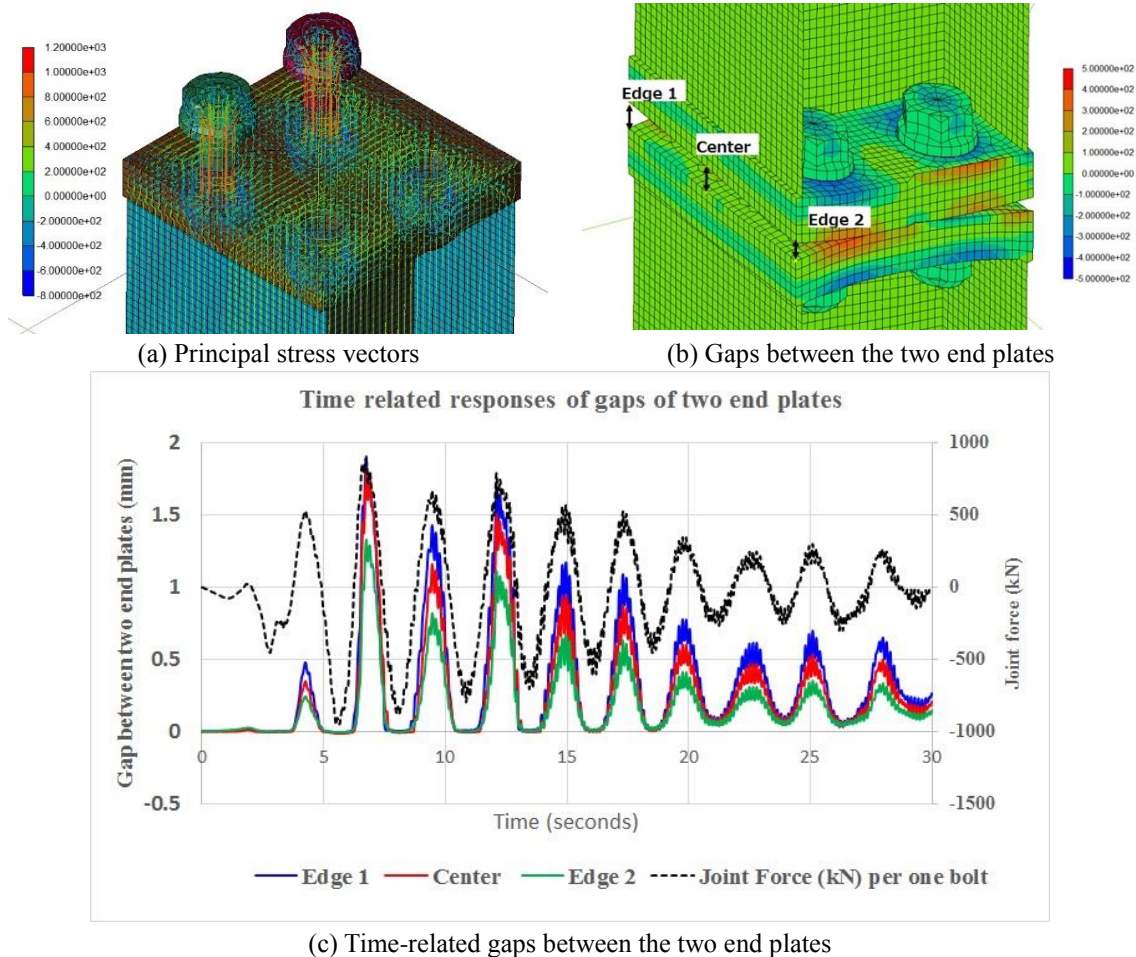(c) Time-related gaps between the two end plates

Fig. 23 Gap between the two end plates and the principal stress vectors

5. Conclusion

By creating a HEM of a tower-crane mast, we could obtain detailed mechanical behavior of the site joints (end-plate-type bolted tensile joints) at the time of an earthquake with a reasonable calculation time using LS-DYNA and a supercomputer. We can replace the detailed joint model portion with a different, alternative joint model that could be used at any joints of the tower-crane mast.

Experiments using specimens are common in studies on the mechanical behavior of joints in steel structures, but they are costly. On the other hand, a computer simulation method can be generally less expensive than experiments when an analytical model that allows more reproducibility and less computation time is devised. In addition, more parameters can be taken into account in the study, so it is an effective method for steel structure joint research.

By using the structural model and simulation method proposed in this paper, it is possible to provide effective information for designing safe joints of tower cranes during earthquakes, taking into consideration workability (control of bolt introduction axial force, etc.) and economy.

Notably, this analysis showed that the joint behavior of the initial pretension axial force of a bolt is considerably reduced after the axial force of the bolt exceeds the yield strength. A maximum decrease of 50% in the initial pretension axial force under the El Centro N–S Wave ($v_{max} = 100$ cm/s) was observed. Results also showed the plastic bending deformation behavior of the large-diameter shafts of the bolts of the end-plate-type bolted tensile joints used herein.

Future studies will use the proposed analysis method by considering parameters such as end-plate thickness, initial pretension axial force of a bolt, bolt strength and diameter, and configuration of bolts to determine the ultimate behaviors of site joints of tower-crane masts during earthquakes and to design safe joints with excellent earthquake resistance. This method can also be applied to analyze the seismic responses of general temporary structures in which joints with lower strength than that of the jointed members are often applied in consideration of the ease of assembly and dismantling. Therefore, the method can contribute to the planning and implementation of earthquake-safety measures on construction sites.

If the study was conducted using this proposed analysis method for constructing the Taipei 101 Building, the behavior of site bolt joints of the tower-crane mast during the catastrophic earthquake could have been determined. However, as a person who experienced this disaster, it can be confirmed that such a study could not be conducted then in consideration of the seismic design standards of the time and the level of technologies in almost 20 years ago.

Acknowledgments

References

Ai, B., Yang, J.L. and Pei, Z.Z. (2013), "Seismic response analysis of tower crane in consideration of the building-crane interaction", *Appl. Mech. Mater.*, **353-356**, 1981-1985

Architectural Institute of Japan (2012), *Recommendation for Design of Connections in Steel Structure*, (Revised in March 2012), Architectural Institute of Japan, Tokyo, Japan.

Chen, C., Lu, T., Chen, H.Y. and Tian, L.C. (2013), "The Finite Element Analysis of Tower Crane Safety Performance", *Appl. Mech. Mater.*, **405-408**, 1135-1158

Gu, Y.Q. and Mao, C.F. (2013), "The preliminary analysis on tower crane by earthquake effect", *Appl. Mech. Mater.*, **353-356**, 1892-1895

Huang, L.J. and Syu, H.J. (2014), "Seismic Response Analysis of Tower Crane Using SAP2000", *Procedia Engineering*, **79**, 513-522

JCAS1101 (2018), Seismic Design Guideline for Cranes, the Japan Crane Association (JCA); Tokyo, Japan.

Loh, C.H., Tsai, K.C., Chung, L.L. and Yeh, C.H. (2003), "Reconnaissance report on the 31 March 2002 earthquake on the east coast of Taiwan", *Earthq. Spectra*, **19**(3), 531-556.

LS-DYNA KUM I (2016), *LS-DYNA Keyword User's Manual Volume I* (LS--DYNA R8.0), JSOL Corporation, Tokyo, Japan.

LS-DYNA KUM II (2016), *LS-DYNA Keyword User's Manual Volume II* (LS-DYNA R8.0), JSOL Corporation, Tokyo, Japan.

Mizushima, Y., Mukai, Y., Namba, H., Taga, K. and Saruwatari, T. (2018), "Super detailed FEM simulations for full-scale steel structure with fatal rupture at joints between members – Shaking table test of full-scale steel frame structure to estimate influence of cumulative damage by multiple strong motion: Part 1", *Jpn. Archit. Rev.*,**1**(1), 96-108

Ushio, Y., Okano, M. and Nagano, Y. (2017), "The earthquake response of climbing-type tower cranes installed in high-rise buildings in consideration of various situation under construction", *Proceedings of 16th World conference on Earthquake Engineering*, Santiago, Chile, January.
Zrnic, N.D., Bosnjak, S.M., Gasic, V.M., Arsic, M.A. and Petkovic, Z.D. (2011), "Failure analysis of the tower crane counterjib", *Procedia Eng.*, **10**(2011), 2238-2243.

CC